Size Effects on Tensile Strength and Fracture Energy In Concrete: Wavelet vs. Fractal Approach

A. Konstantinidis[1], G. Frantziskonis[2], A. Carpinteri[3] and E.C. Aifantis[1,4]

[1]*Laboratory of Mechanics and Materials, Polytechnic School, Aristotle University of Thessaloniki, GR -54006, Thessaloniki, Greece*
[2]*Dept. of Civil Engineering and Engineering Mechanics, University of Arizona, Tucson, AZ 85721, USA*
[3]*Dept. of Structural Engineering, Politecnico di Torino, IT-10129, Torino, Italy*
[4]*Center for Mechanics of Materials and Instabilities, Michigan Technological University, Houghton, MI 49931, USA*

ABSTRACT

The problem of size effect on tensile strength and fracture energy of brittle, heterogeneous and disordered materials is considered within two, apparently different approaches: one based on wavelets and scale-dependent constitutive relations and another based on fractal arguments. Using wavelet analysis, scale-dependent constitutive relations are derived from an underlying gradient formulation. By varying the scale parameter, size effects in tensile strength and fracture energy can be captured. Using fractal analysis, a fractal dimension of the damaged material surface which the stress acts upon is defined and a corresponding size-dependent tensile strength and fracture energy is obtained. These two approaches are then compared. Both of them give results with similar trend and their divergence emerges only in the limit of infinitesimally small specimens, where different deformation mechanisms and random responses may prevail.

1. INTRODUCTION

The heterogeneity inherently present in most engineering materials and revealed at certain length scales is of primary importance in defining material behavior and interpreting some usual properties such as size effects. Metals with fine grain microstructure exhibit measurable size effects at very small scales (~ μm) with an asymptotic behavior at larger ones, while concrete typically shows measurable size effects at relatively larger scales of the order of aggregate size (~ cm), with an asymptotic behavior at even larger scales.

In the field of mechanics of materials, spatial interaction and heterogeneity effects can be effectively represented within a continuum formulation by introducing a length scale directly into constitutive equations.

For example, Aifantis /1/ has suggested the so-called gradient theory in order to include internal length scales into the constitutive relations. In this approach, higher order spatial gradients of strain (e.g. the Laplacian of the elastic strain tensor – or the Laplacian of the plastic strain intensity) or internal variables were incorporated in the constitutive equations and subsequent stability analysis providing a means for estimating wavelengths of dislocation cells, widths and spacings of shear bands, as well as a mechanism for eliminating the mesh-size dependence of finite element calculations in the material softening regime (for an account of these developments, the reader may consult the recent reviews by Aifantis /2-5/ and the references quoted therein). An additional effect that the gradient theory seems to capture is the dependence of mechanical properties (e.g. yield stress, failure stress) on the size of the specimen. This was outlined initially by Aifantis /6/ for plastically twisted wires and elastically pressurized boreholes of varying diameter (see also his more recent contribution on this subject /7/) and later by Zhu *et al* /8/ for metal-matrix particulate composites with varying reinforcement size.

An alternative approach to incorporate length scales into the constitutive equations is outlined in a recent study by Frantziskonis and Loret /9/ who utilized the shear band solution of gradient theory /1,2/ to calibrate a wavelet-based constitutive equation, thus replacing the gradient term $\nabla^2\gamma$ for the equivalent plastic strain γ with a scale parameter s. By varying the scale parameter s different stress-strain relations were obtained. This wavelet-based gradient approach was shown in a preliminary study by Frantziskonis *et al* /10/, as well as by Tsagrakis *et al* /11/, to be able to capture size-effects in tensile strength and toughness, in qualitative agreement with available experimental data and a related fractal approach to size effects described below.

The aforementioned fractal formulation for addressing the problem of size effects on tensile strength and fracture energy is based on the fractal nature of material ligament and fracture surface and was proposed by Carpinteri /12/. The reacting section or ligament in a disordered material at peak stress is represented as a fractal space of dimension $2\text{-}d_\sigma$, where d_σ is a dimensional decrement that might be due to the presence of voids and cracks and, in general, to any material inhomogeneity leading to a cross-sectional weakening. Also the fracture surfaces of metals and concrete show a fractal character and have a dimension $2+d_G$, where d_G is a dimensional increment representing the attenuation of fracture localization due to material heterogeneity and multiple cracking. The approach provides two so-called multi fractal scaling laws (MFSL) for interpreting size effects in tensile strength and fracture energy, respectively.

In the present paper we review both the wavelet-based and fractal-based approaches and compare them with respect to addressing the problem of size effect in concrete specimens subjected to tension; in particular, with respect to size-dependence of strength and fracture energy. The wavelet-based approach is described in Section 2, while the fractal-based approach is described in Section 3. Explicit relations for the size-dependence of both tensile strength and fracture toughness are provided for both approaches. Finally, in Section 4 the two approaches are compared with respect to each other, as well as with respect to experimental data.

2. WAVELET-BASED GRADIENT APPROACH

2.1. Wavelet Analysis and Scale-dependent Constitutive Equations

Wavelet analysis provides a tool to represent functions in space and scale with a few parameters commonly known as wavelet coefficients. The wavelet transform is an integral transform that decomposes an input signal into amplitudes depending on position and scale by using simple base functions commonly known as wavelets. By changing the scale of the wavelet, relevant information is provided at higher and higher resolution at a certain location in space /13/. The set of base functions (wavelets) are chosen to be well-localized (of compact support) both in space and frequency, thus providing dual-localization properties. This set is constructed from a single function $\psi(x)$, the so-called "mother" wavelet, i.e.

$$\psi_{\alpha,b}(x) = \psi\left(\frac{x-b}{\alpha}\right), \tag{1}$$

where $\alpha > 0$ is a scale parameter and $-\infty < b < \infty$ is a translation parameter. For a given function f(x), the wavelet coefficients are calculated from the relation

$$W[f](\alpha,b) = \frac{1}{\sqrt{\alpha}} \int_{-\infty}^{\infty} f(x)\psi_{\alpha\, b}(x)\,dx\,. \tag{2}$$

It is possible to reconstruct the function from the wavelet coefficients through the inversion formula

$$f(x) = \frac{1}{c_\psi} \int_0^\infty \int_{-\infty}^{\infty} W[f]\psi_{a,b}(x)\,db \qquad \frac{da}{a^2}, \tag{3}$$

where c_ψ is a coefficient evaluated from the wavelet ψ. By replacing the lower limit of integration in the first integral of (3) by s, we obtain the representation of f up to scale s herein denoted as $f_s(x)$, i.e.

$$f_s(x) = \frac{1}{c_\psi} \int_s^\infty \int_{-\infty}^{\infty} W[f]\psi_{a,b}(x)\,db \qquad \frac{da}{a^2}. \tag{4}$$

The above mathematical ideas may be used to derive scale-dependent constitutive equations by utilizing a shear band solution obtained within the gradient plasticity theory of Aifantis /1,2/ as discussed by Frantziskonis and co-workers /9,10/ and also by Tsagrakis *et al* /11/. In fact, a length scale incorporated into constitutive equations may be thought of as representing the range of appreciable material interactions. It follows that this range diminishes just prior to fracture initiation at a certain fracture location point (for 1-D problems), while it may still be appreciable at other locations of the specimen or structure at hand. As shown in the recent work of Frantziskonis *et al* /10/ and Tsagrakis *et al* /11/, the strain localization zone may be approximated by the wavelet representation of the δ-function up to scale s, denoted as δ_s. By using an appropriate "mother wavelet" that yields physically appealing shapes for the localization zone, i.e.,

$\psi(x) = x\ \mathrm{Exp}(-x^2/2)$, the aforementioned wavelet representation of the δ-function δ_s used in the present paper reads

$$\delta_s = \frac{1}{\sqrt{\pi}} \frac{s_0}{2s\ \mathrm{Exp}\left[\frac{x^2}{4s^2}\right]}, \tag{5}$$

where s denotes the scale such that $0 < s < \infty$, with zero representing the limit approached at very fine scales. The additional parameter s_0 may be viewed as the amplitude of the δ function used in order to approximate strain localization zones in different materials. More precisely then, δ_s in (5) is the representation of $s_0\delta(x)$ at scale s. Thus, from the wavelet-based representation of the localization zone, the strain profile may be captured in increasing or decreasing level of detail depending on the value of the scale parameter s used. Various profiles of strain localization zones described by (5) are shown in Figure 1 for different values of the scale parameter s.

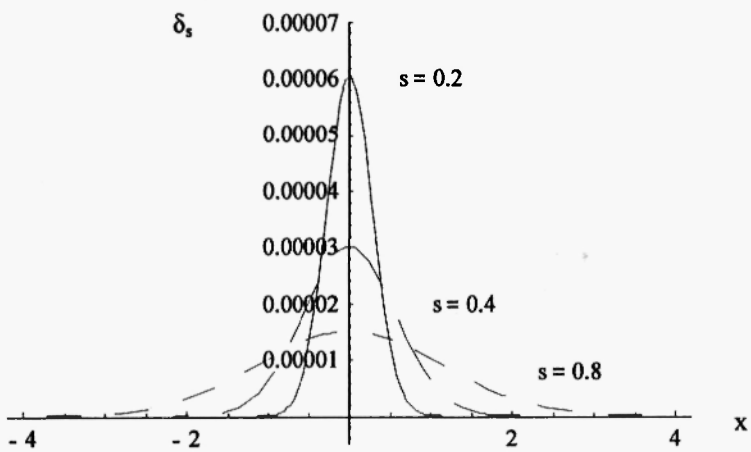

Fig. 1: Plot of (5) for different values of s

The governing equilibrium and gradient-dependent constitutive equation describing the shape of the localized deformation or damage zone for one-dimensional tension read

$$\frac{\partial\sigma}{\partial x} = 0 \quad , \quad \sigma_0 = \kappa(\varepsilon) - c\frac{\partial^2\varepsilon}{\partial x^2} \Rightarrow \sigma_0 = \kappa(\varepsilon) - c\frac{\partial^2\varepsilon}{\partial x^2} \tag{6}$$

where ε denotes tensile strain, $\kappa(\varepsilon)$ is the constitutive response of the "background" homogeneous material, σ_0 is the applied tensile stress, and c denotes the so-called gradient coefficient with dimensions of force. Given the explicit form of the function $\kappa(\varepsilon)$, elegant analytical solutions of (6)$_3$ in the form of localized

deformation bands can be obtained in a manner similar to that done for one-dimensional shear deformation and shear bands by Aifantis /1,2/ and in more detail by Zbib and Aifantis /14,15/. We may evaluate $\kappa(\varepsilon)$ by assuming that (5) approximates the strain profile within the localization zone whose evolution is determined by the scale s which, in turn, decreases during deformation and approaches zero at the onset of fracture. This assumption is justified in the recent work of Frantziskonis *et al* /10/ and Tsagrakis *et al* /11/ where the problem of size effects and scale-dependent constitutive equations through wavelet analysis is also considered. In passing, we note that the background response $\kappa(\varepsilon)$ is difficult to measure experimentally, for softening response (Bazant and Pijaudier-Cabot, 1989), since it is difficult to "force" specimens to deform uniformly.

Next we eliminate the gradient term from (5) and (6) by making the identifications $\delta_s \rightarrow \varepsilon - \varepsilon_\infty$ and $s \rightarrow c_s s$ where ε_∞ denotes the "homogeneous" strain at the specimen's ends (which are assumed to be at "infinite" distance from the localized deformation zone such that the train gradient vanishes there) and the new material parameter c_s is introduced to account for the rate of change in scales during deformation for a specific material. Without loss of generality for the arguments to follow we may formally take ε_∞ to vanish since the difference $\varepsilon - \varepsilon_\infty$ representing the strain difference inside and outside the localization zone increases rapidly at advanced straining stages where the fracture stress and toughness (which are of interest here) are to be evaluated. We further assume that the gradient-independent term $\kappa(\varepsilon)$ in (6) associated with a homogeneously deforming specimen corresponds to the scale-dependent local stress $\sigma(\varepsilon,s)$ of an inhomogeneously deforming specimen at the strain level ε. As a result we obtain the following scale-dependent expression for the stress

$$\sigma(\varepsilon,s) = \sigma_0 - \frac{c\,\varepsilon}{2\,c_s^2\,s^2}\left(2\mathrm{Log}\left[2\sqrt{\pi}\,\frac{c_s\,s}{s_0}\,\varepsilon\right] + 1\right), \tag{7}$$

valid for the non-elastic portion of the stress-strain diagram. The value σ_0 corresponds to a zero value of inelastic strain. The elastic strain, which is related to the stress through the usual linear elasticity relation, can be incorporated into the above formulation in a straightforward manner, but this is not needed in the following analysis. It is also noted that while σ_0 in (6) coincides with the applied stress, its meaning in (7) is more general and, as it will be seen later, it corresponds to the nominal strength of an infinitely large specimen for which scale effects are insignificant.

Finally, it should be pointed out that the gradient coefficient c in (7) is basically a force acting on a surface s^2. Thus, in order to utilize the above equation to address the problem of size effects in the 2-D similitude experiments by Carpinteri and Ferro /16/ where the nominal area is given by sb (b is the specimen's thickness) and only one of the sides (width) is scaled the substitution $c_s^2 s^2 \rightarrow c_s s\,b$ should be made. Then, (7) takes the form

$$\sigma(\varepsilon,s) = \sigma_0 - \frac{c\,\varepsilon}{2c_s\,s\,b}\left(2\mathrm{Log}\left[2\sqrt{\pi}\,\frac{\sqrt{s\,c_s b}}{s_0}\,\varepsilon\right] + 1\right), \tag{8}$$

which will be used next to model the size-dependence of strength and toughness of concrete specimens in tension. It is emphasized that (8) is a stress-strain relation incorporating in addition to the scale and material parameters, also the specimen thickness b and the applied stress σ_0 at the boundary where the deformation is uniform. The scale parameter s is identified with the specimen size, which is used to scale the gage length used to determine the specimen's strength. In this context, (8) is not a constitutive equation in the usual sense but a relationship modeling the strength of a particular specimen with given geometric characteristics. The stress σ_0 is the value of the scale-independent homogeneous component of stress experienced by the uniformly deforming parts of the specimen far from the localization zone and in our case coincides with the applied stress. It turns out that for long specimens with infinitely large values of s, σ_0 is the actual strength of the specimen since no localization effects can be detected with the gage length used. For smaller specimens where smaller gage lengths are used, localization effects are detected and they become important in determining the maximum value of the local stress σ given by (8) which now should be identified with the actual strength of the specimen at hand.

2.2. Application to Size Effects on Nominal Strength and Fracture Energy

In this section, the scale-dependent constitutive relations derived previously are applied to model size effects on tensile strength and fracture energy. From (8) it follows that

$$\lim_{s\to\infty} \sigma(\varepsilon, s) = \sigma_0 . \tag{9}$$

Then, since up to the peak stress, i.e. before initiation of localization, the scale parameter s remains constant and equal to the specimen width d, (9) implies that σ_0 is the nominal strength of a bar of infinite length. By setting the derivative with respect to ε equal to zero in (8), the strain at the peak stress, denoted as ε_{peak}, is obtained. Then, substituting ε_{peak} for ε in (8) yields the peak stress σ_{peak}. The corresponding two relationships read

$$\varepsilon_{peak} = \frac{s_0}{2\mathrm{Exp}[3/2]\sqrt{\pi}\sqrt{c_s \quad s\, b}} \rightarrow \sigma_{peak} = \sigma_0 + \frac{s_0\, c}{2\mathrm{Exp}[3/2]\sqrt{\pi}(s\, c_s\, b)^{3/2}} . \tag{10}$$

Fracture energy is defined as $G_f = W_F / A_0$, where W_F denotes the total work necessary for complete fracture and A_0 is the initial resisting area. It is traditionally considered as a material constant representing a local quantity obtained from an (unspecified) averaging process representing the mean effects of the microstructure in the material. Within the context of scale-dependent constitutive relations, fracture toughness is evaluated as

$$G_f = \int\int \sigma d\varepsilon dx \tag{11}$$

where the integral is evaluated over the entire strain path and along the length of the considered one-dimensional specimen; i.e. a bar under tension for the present case. Thus,

$$G_f = \int_{-L/2}^{L/2} \int_{s_f}^{s_c} \sigma(\varepsilon, s) \frac{d\varepsilon}{ds} ds dx \quad (12)$$

where L is the length of the bar, containing a localization zone in the middle, and s_f, s_c are the finest and coarsest scales used. It is assumed that the finest scale s_f is approximately equal to the maximum grain size of the concrete specimens and that the coarsest scale s_c is equal to the specimen width (the dimension scaled in the 2-D similitude). When the scale s is equal to the finest scale s_f, it is implied that the behavior of a bar with only one large aggregate is controlled by the behavior of the aggregate itself. Furthermore, at the initiation of straining, the scale parameter s appearing in (8) is equal to the bar width d; in other words, since the largest scale in the problem is the bar size, scales larger than that are not activated.

Since in the series of experiments examined in Section 4, a constant ratio L/d=4 (L,d: specimen length and width, respectively) was selected, we used this ratio for evaluating G_f from (12) for all specimens. Upon direct integration of (12) by using the program Mathematica™, we obtain

$$G_f = \frac{s_0\left(2s_0 bcc_s s_f e^{-2d/bc_s}\left(-bc_s s_f - 2ds_f - 2d^2 s_f\right) + 2cs_0 e^{-2d^2/bc_s s_f}\left(2d^4 + 2bc_s d^2 s_f + b^2 c_s^2 s_f^2\right) + A\right)}{32\pi b^2 c_s^2 d^3 s_f^2}, \quad (13)$$

where

$$A = 32b^2 c_s^2 d^2 s_f^2 \pi\sigma_0 \left(\mathrm{Erf}\left[\sqrt{\frac{d}{bc_s}}\right] - \mathrm{Erf}\left[\frac{d}{\sqrt{bc_s s_f}}\right]\right) - \sqrt{2\pi bc_s}\, cd^{3/2} s_f^2 s_0 \left(\mathrm{Erf}\left[\sqrt{\frac{2d}{bc_s}}\right] - \mathrm{Erf}\left[\frac{\sqrt{2}d}{\sqrt{bc_s s_f}}\right]\right),$$

and Erf/./ denotes the error function.

3. MULTIFRACTAL APPROACH

3.1. Fractal Analysis of Material and Fracture surfaces in Tensile Tests

Fractal sets appearing in nature show random self-similar morphologies, i.e. they show statistical similarity under changes in the scale of observation. In all such natural fractal structures there is an upper and a lower bound limiting the scaling regime; thus a transition from the fractal (disordered) regime at the microscopic level towards the Euclidean (homogeneous) regime at the largest scales takes place. The upper bound is represented by the macroscopic size of the set, while the lower bound is related to the size of the smallest measurable particles, e.g. aggregates in the case of concrete. The aforementioned transition, first pointed out by Mandelbrot /17/, for a variety of physical phenomena, has been verified experimentally by Carpinteri /18/ and Carpinteri and Chiaia /19/ in the case of fracture of concrete.

It is assumed that the reacting section or ligament of a disordered material at peak stress is represented as a lacunar fractal space of dimension $2-d_\sigma$, with $0< d_\sigma<1$. This dimensional decrement may be attributed to the presence of voids and cracks and, in general, to any material inhomogeneity that leads to cross-sectional weakening. On the other hand, the fracture surfaces of materials such as metals and concrete present an invasive fractal nature and have a dimension of $2+d_G$, where d_G is a dimensional increment representing the attenuation of fracture localization due to material heterogeneity and multiple cracking. These two assumptions lead to a "renormalized" tensile strength σ_u^* and a "renormalized" fracture energy G_F^* which are material constants /12/. Moreover, it can be shown that the highest possible disorder in the microstructure is represented by a Brownian disorder, i.e. a fractal dimension equal to 2.5, seems to be the highest in the limit of microscopic scales of observation. The experimental determination of the size-effect exponents to be discussed later, either in the case of tensile strength (e.g. Carpinteri and co-workers /20,21/) or in the case of fracture energy (e.g. Carpinteri and Chiaia /19,22/), for which the absolute values have never been measured to be larger than 0.5, is an indirect validation of the considerations presented above.

3.2. Multifractal Scaling Laws for Tensile Strength and Fracture Energy

Since, within the aforementioned fractal framework, one may assert the existence of true material parameters for the strength σ_u^* and the fracture energy G_F^* which are invariant under a change of scale, one may derive explicit expressions for the size-dependence of the apparent or nominal strength and fracture energy. As will be seen below, these expressions reflect the influence of disorder on the mechanical properties through the ratio between a characteristic length ℓ_{ch} and the external size d of the specimen. Thus, the effect of microstructural disorder becomes progressively less important at larger scales, whereas it represents a fundamental feature at smaller ones.

A statistical size distribution of defects may be defined for which the most dangerous one proves to be of size proportional to the structural size. This corresponds to materials possessing a considerable dispersion in the statistical microcrack size distribution (disordered materials). In this case, the power of the Linear Elastic Fracture Mechanics (LEFM) stress singularity, ½, turns out to be the slope of the graph providing the decrease of tensile strength vs. specimen size in a bilogarithmic diagram. When the statistical dispersion is relatively low (ordered materials) the slope is less than ½ and tends to zero for regular distributions (perfectly ordered materials). Analogous considerations can also be made for the fracture energy. In particular, a Brownian disorder is assumed to be the highest possible disorder at the smallest scales yielding fractional scaling exponents equal to −0.5 for lacunar (tensile strength ligaments) and to 0.5 for invasive (fracture energy surfaces) topologies.

Based on the above assumptions, two Multifractal Scaling Laws (MFSL) have been proposed for tensile strength and fracture energy with the following analytical form (Carpinteri /18/):

$$\sigma_u(d) = f_t\left(1+\frac{\ell_{ch}}{d}\right)^{1/2}, \tag{14}$$

for the tensile strength, and

$$G_F(d) = G_F^{\infty}\left(1+\frac{\ell_{ch}}{d}\right)^{-1/2}, \tag{15}$$

for the fracture energy. In (14) and (15) $f_t, G_F^{\infty}, \ell_{ch}$ denote the lowest nominal tensile strength, the highest nominal fracture energy and the characteristic length, respectively. The asymptotic values of the two laws (f_t, G_F^{∞}) is reached only in the limit case of a specimen with infinite size. The bracketed terms represent the variable influence of disorder on the mechanical behavior. It should be noted here that the bilogarithmic plot of these Multifractal Scaling Laws shows a slope of –0.5 and 0.5 in the limit of very small specimens for tensile strength and fracture energy, respectively.

4. COMPARISON OF THE TWO APPROACHES WITH EXPERIMENTS

In this section both of the above approaches are used to interpret experimental data on size effects obtained earlier by Carpinteri and co-workers /21/ on concrete specimens. The specimens were flared in the center and their thickness was constant and equal to 10 cm, while the ratio of specimen length to specimen width was 4:1. The scale range was 1:16 and tests were carried out on four specimen sizes; the dimensions of the cross section were 2.5×10 cm^2, 5×10 cm^2, 10×10 cm^2, 20×10 cm^2, and 40×10 cm^2. The test specimens were glued to steel supporting plates in order to be attached to the load-bearing system. The concrete mix had a water-cement ratio of 0.5 and the maximum gravel size was 16 mm.

The experimental data were first fitted within the framework of the wavelet-based gradient approach. The fitting was made using the nonlinear fitting routine of Mathematica™, which is based on a Levenberg-Marquardt algorithm. The nonlinear fitting provided the following values for the various coefficients: $\sigma_0 = 3.84$ MPa, $c_s = 0.0193$, $s_0 = 0.318$ mm, $c = 17.76$ kN. If a value of 30 GPa is assumed for the Young's modulus E of the concrete specimens, then the internal length provided by the gradient theory is equal to $\ell = \sqrt{c/E} = 0.77$ mm; note that this value is small compared to the size of the aggregates, since it represents the scale dominating the localization process at the later stages, i.e., close to complete fracture. It should be noted that the specimen thickness was constant and equal to 10 cm and the finest scale was taken to be approximately equal to the maximum gravel size, i.e. 16 mm.

The corresponding fitting with the Multifractal Scaling Laws gave the following values for the various coefficients: $f_t = 3.68$ MPa and $\ell_{ch} = 19.3$ mm for the tensile strength law and $G_F^{\infty} = 318.86$ N/m and $\ell_{ch} = 93.9$ mm for the fracture energy law.

It should be noted that for the fitting was done using the mean values of the experimental observations. Furthermore, for both approaches some data were not included due to the fact that the corresponding experimental measurements for these points were not accurate. The comparison between the two approaches is shown in Figures 2 to 5; in Figures 2,3 the variations of tensile strength and fracture energy vs. size are shown, while in Figures 4,5 the corresponding bilogarithmic diagrams are given.

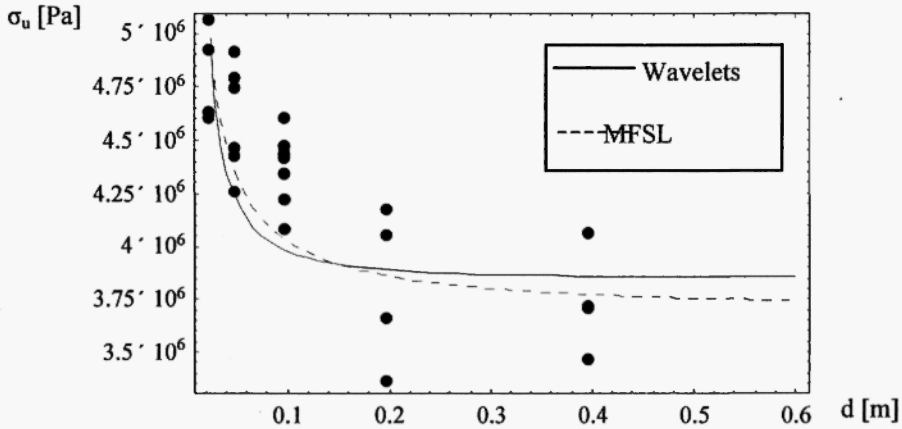

Fig. 2: Comparison for the tensile strength data

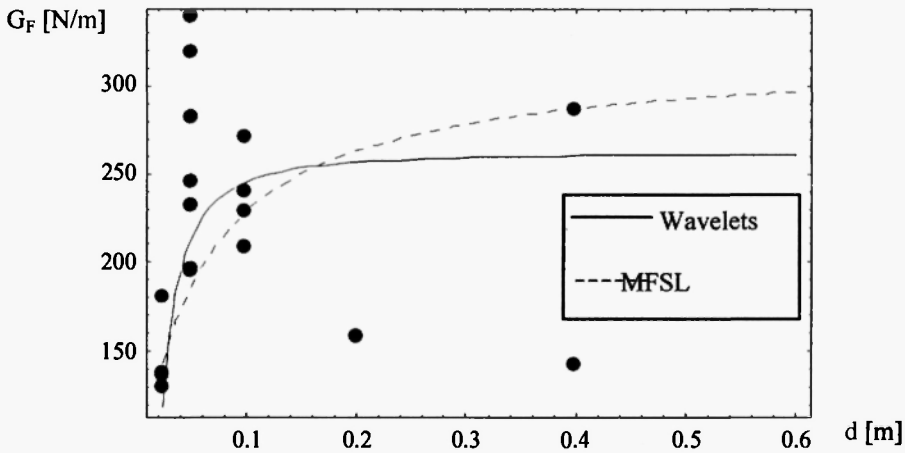

Fig. 3: Comparison for the fracture energy data

From the above figures it can be seen that both approaches show similar trends in predicting size effects. As mentioned previously, their divergence emerges in the limit of very small specimens. At that limit, in the bilogarithmic diagrams the slopes for the tensile strength and the fracture energy provided by the wavelet-based gradient approach are greater in absolute value than the corresponding ones given by the Multifractal Scaling Laws. This divergence is to be expected due to the completely different arguments on which the two approaches are based. For the MFSL and in the limit of infinitesimally small specimens the respective slopes of –½ and ½ in the bilogarithmic diagrams for tensile strength and fracture energy, are imposed at the outset as a requirement of Griffith's Theory. In contrast, in the wavelet-based gradient approach such a restriction is

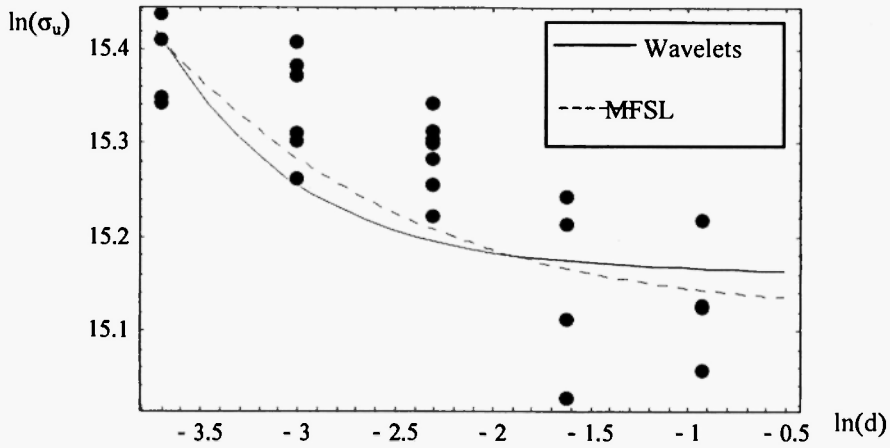

Fig. 4: Bilogarithmic comparison for the tensile strength data

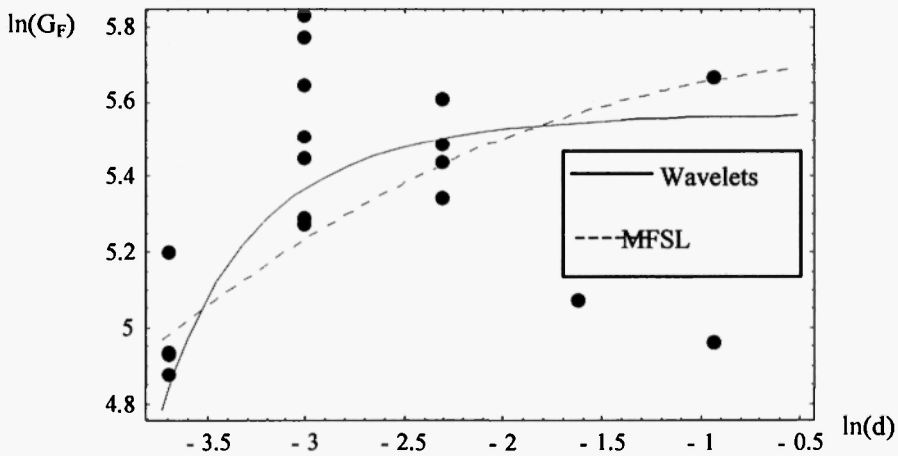

Fig. 5: Bilogarithmic comparison for the fracture energy data

not required, even though a physically imposed cutoff distance s_f is used. The fact, however, that both approaches show the same trends in addressing the problem of size effects is rather interesting. Furthermore, it should be noted that the aforementioned divergence emerges in a limit case, which may not be captured by either approach, since different deformation mechanisms and completely random responses may prevail at such small scales.

ACKNOWLEDGEMENTS

The financial support of the European Union under program TMR, contract n° FMRX-CT96-0062 is acknowledged. The second and fourth author also acknowledge the support of the US National Science Foundation.

REFERENCES

1. Aifantis E.C., 1984, On the microstructural origin of certain inelastic models, *Trans. ASME, J. Eng. Mat. Techn.* **106**, 326-330.
2. Aifantis E.C., 1987, The physics of plastic deformation, *Int. J. Plasticity* **3**, 211-247.
3. Aifantis E.C., 1992, On the role of gradients in the localization of deformation and fracture, *Int. J. Engng. Sci.* **30**, 1279-1299.
4. Aifantis E.C., 1995, Pattern formation in plasticity, *Int. J. Engng. Sci.* **33**, 2161-2178.
5. Aifantis E.C., 1999, Gradient deformation models at nano, micro, and macro scales, *J. Engng. Mat. Techn.* **121,** Trans. ASME, 189-202.
6. Aifantis E.C., 1996, Higher order gradients and size effects, In *Size-Scale Effects in the Failure Mechanisms of Materials and Structures*, ed. A. Carpinteri, pp. 231-242, E & FN Spon, London.
7. Aifantis E.C., 1999, Strain gradient interpretation of size effects, *Int. J. Fracture* **95,** 299-314.
8. Zhu H.T., Zbib H.M. and Aifantis E.C., 1997, Strain gradients and continuum modeling of size effect in metal matrix composites, *Acta Mechanica* **121**, 165-176.
9. Frantziskonis G. and Loret B., 1995, Scale dependent constitutive relations - information from wavelet analysis and application to localization problems, *Eur. J. Mech., A / Solids* **14**, 873-892.
10. Frantziskonis G., Konstantinidis A. and Aifantis E.C., 2000, Scale-dependent constitutive relations and the role of scale on nominal properties, *Eur. J. Mech. A/Solids* accepted.
11. Tsagrakis I., Konstantinidis A. and Aifantis E.C., 1999, Strain gradient and wavelet interpretation of size effects in yield and strength, *preprint*.
12. Bazant, Z.P. and Pijaudier-Cabot, G., 1989, Measurement of characteristic length of nonlocal continuum, J. of Eng. Mech. ASCE **115** , 755--767.
13. Carpinteri A., 1994, Fractal nature of material microstructure and size effects on apparent mechanical properties, *Mech. Mater.* **18**, 89-101; also in Internal Report 1/92, Dept. Struct. Eng., Politecnico di Torino, Torino, Italy (1992).
14. Daubechies I., 1992, *Ten lectures on wavelets*, SIAM, Philadelphia, Pennsylvania.
16. Zbib H.M. and Aifantis E.C., 1988, On the localization and postlocalization behavior of plastic deformation. II. On the evolution and thickness of shear bands, *Res Mechanica* **23**, 279-292.
17. Zbib H.M. and Aifantis E.C., 1992, On the gradient-dependent theory of plasticity and shear banding, *Acta Mechanica* **92**, 209-225.

18. Carpinteri A. and Ferro G, 1994, Size effects on tensile fracture properties: a unified explanation based on disorder and fractality of concrete microstructure, *Mater. Struct.* **27**, 563-571.
19. Mandelbrot B.B., 1985, Self-affine fractals and fractal dimension, *Phys. Scr.* **32**, 257-260.
20. Carpinteri A., 1994, Scaling laws and renormalization groups for strength and toughness of disordered materials, *Int. J. Solids Struct.* **31**(3), 291-302.
21. Carpinteri A. and Chiaia B., 1995, Multifractal nature of concrete fracture surfaces and size effects on nominal fracture energy, *Mater. Struct.* **28**, 435-443.
22. Carpinteri A., Chiaia B. and Ferro G., 1995a, Size effects on nominal tensile strength of concrete structures: multifractality of material ligaments and dimensional transition from order to disorder, *Mater. Struct.* **28**, 311-317.
23. Carpinteri A., Chiaia B. and Ferro G., 1995b, Multifractal scaling law: An extensive application to nominal strength size effect of concrete structures, Report 51, Dept. Struct. Eng., Politecnico di Torino, Torino, Italy.
24. Carpinteri A. and Chiaia B., 1996, Size effects on concrete fracture energy: dimensional transition from order to disorder, *Mater. Struct* **29**, 259-266.